Periodic Orbits in Generalized Mushroom Billiards
SURF 2006 - Final Report

Kris Kazlowski

kkaz@caltech.edu

(Dated: October 30, 2006)

Abstract: A mathematical billiard consists of a closed domain of some shape with a confined point particle moving with constant speed and colliding elastically against its boundary. Depending on the billiard geometry, it can exhibit chaotic, regular, or mixed regular-chaotic dynamics. Because mixed systems are more difficult to analyze than fully chaotic or fully regular ones, it is important to study simple examples that can be investigated precisely. To provide useful insights into mixed systems, we consider periodic orbits in billiards shaped like mushrooms and generalizations thereof. Using a combination of analytical and numerical techniques, we obtain conditions for stability (primarily for orbits of periods two and four, but with a few results for orbits with higher periods) as functions of table dimensions.

In this paper, we study periodic orbits in billiards with mixed regular-chaotic dynamics using analytical and numerical methods. We investigate, in particular, the elliptical mushroom, which is shaped like a rectangle with a semi-elliptical cap on one end. We also study the double elliptical mushroom, which has caps on both ends. Although fully integrable and chaotic systems are well-understood, mixed systems are very poorly understood. Consequently, simple examples like those studied here can provide tremendous insights into the dynamics of mixed systems.

INTRODUCTION

Billiards are dynamical systems that arise from a mathematical idealization of the familiar game of billiards. They are of considerable interest to both mathematicians and physicists, as they have led to numerous discoveries in fields such as ergodic theory [8]. Additionally, an understanding of billiards can lead to insights in applications such as the problem of hearing the shape of a drum [10]. Moreover, billiards have been constructed experimentally using microwave cavities [12], ultracold atoms [11], and other settings.

A billiard table is a compact domain $Q \subset R^n$ (in this study, $n = 2$). A billiard system consists of a table with a confined point particle moving with constant speed and colliding perfectly elastically against its boundary. Studying the periodic orbits of a billiard provides insight into its dynamics, which can be chaotic, regular (non-chaotic), or a mixture of the two. A chaotic billiard is one in which initially nearby trajectories diverge at an exponential rate, as they depend sensitively on their initial positions and velocities because of the billiard geometry. The stadium and Sinai billiards are canonical examples of chaotic billiards. The stadium consists of a rectangle with a semicircle on each end instead of a line segment, and the Sinai billiard table is a square with a circle in the middle [8]. A billiard is regular (roughly, integrable) when its paths do not depend sensitively on initial conditions. More precisely, an integrable system possesses as many constants of motion as degrees-of-freedom (position-momentum pairs). For example, circular and elliptical billiards are both integrable.

A circular mushroom billiard consists of a semicircular cap attached to a stem of some shape (see Figure 1a) [6]. Circular mushroom billiards provide a smooth transition between integrable semicircular billiards and chaotic semistadium billiards as the width of the stem is increased from zero to the diameter of the circle. An elliptical mushroom billiard is similar, except the cap is semi-elliptical rather than semicircular. It is sometimes also convenient to consider double mushrooms, which are mushrooms with caps on both ends of the stem (see Figure 1b). In Figure 1a, the red trajectories are non-chaotic and the black ones are chaotic. For circular mushrooms with rectangular stems, all paths from the cap that enter the stem are chaotic (except for a set of measure zero), and all paths that remain in the cap are regular. Hence, this system has mixed regular-chaotic dynamics. The billiard geometry can be characterized using only two parameters: the height and width of the rectangle (with the radius of the semicircle fixed to 1).
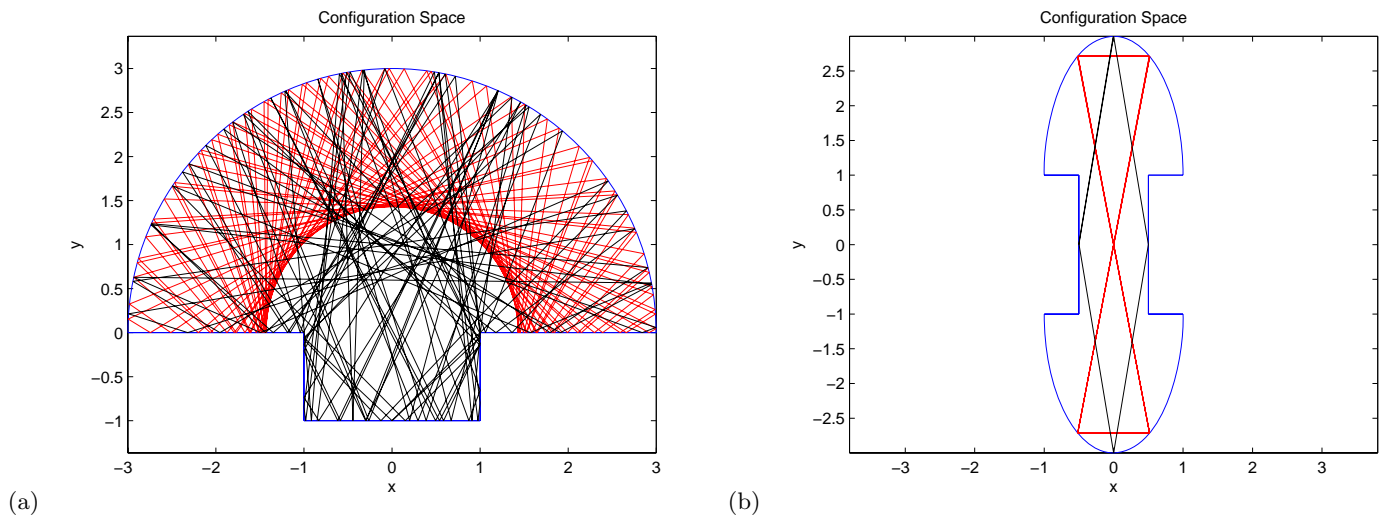
FIG. 1: **(a)** Configuration space of a circular mushroom billiard. The red trajectories are regular and the black ones are chaotic. **(b)** Double elliptical mushroom billiard, with diamond (black) and bowtie (red) orbits shown.

RESULTS AND DISCUSSION

We study single and double symmetric elliptical mushroom billiards with rectangular stems. These tables are parametrized by the height and width of the rectangle and the lengths of the semimajor and semiminor axes. We investigate the dynamics and stability of periodic orbits as a function of these parameters using Poincaré maps and stability (Jacobian) matrices.

Important Concepts

Jacobian Matrices

The coordinates of one collision with the boundary can be mapped to those of the next using a billiard map f: $x_{n+1} = f(x_n)$. A periodic orbit of period k satisfies $x = f^{(k)}(x)$ for all points x on the orbit and does not satisfy $x = f^{(i)}(x)$ for $i < k$. That is, k is the smallest integer j such that $f^{(j)}(x) = x$. One can visualize the billiard's "phase space" (describing its position vs. angle of collision) from these successive x_n, by plotting the arc length versus incident angle for each x_n.

Jacobian matrices arise from considering what happens to a trajectory (such as a periodic orbit) when it is perturbed a small amount, δx. One expands in a Taylor series.

$$f(x_0 + \delta x) = f(x_0) + f'(x_0)\delta x + \frac{f''(x_0)(\delta x)^2}{2!} + \ldots + \frac{f^{(n)}(x_0)(\delta x)^n}{n!} + \ldots \qquad (1)$$

For sufficiently small δx one can approximate (1) by keeping only the linear terms. That is,

$$f(x_0 + \delta x) \approx f(x_0) + f'(x_0)\delta x.$$

This yields a Jacobian matrix, describing the (linear) dynamics of the perturbation [4]. We calculate its eigenvalues as a function of the system parameters to see whether or not an orbit is stable.

One obtains the Jacobian matrix for a billiard's periodic orbit by taking a product of matrices corresponding to the free flight and collisions with the boundary for a particular orbit. One then determines its stability by examining its

eigenvalues. Because the Jacobian matrix has two eigenvalues and billiard systems are Hamiltonian, if both eigenvalues have a magnitude of 1, then the orbit is stable. The eigenvalues are, by definition, factors of growth of the deviations after applying the mapping. Under repeated iterations of the billiard map, deviations increase by the eigenvalues raised to some exponent. After j iterations, we get the deviations

$$\begin{pmatrix} \delta s_j \\ \delta p_j \end{pmatrix} = A\lambda_+^j \begin{pmatrix} \delta s_+ \\ \delta p_+ \end{pmatrix} + B\lambda_-^j \begin{pmatrix} \delta s_- \\ \delta p_- \end{pmatrix} \tag{2}$$

where s is arc length, p is momentum, and A and B are some constants [5]. The deviation in arc length after j iterations is δs_j, and so forth.

One can show that a periodic orbit is stable if and only if $|Tr(J)| \leq 2$ [5]. In terms of $Tr(J)$, the eigenvalues are

$$\lambda_\pm = \frac{1}{2}\{Tr(J) \pm [(Tr(J))^2 - 4]^{\frac{1}{2}}\}. \tag{3}$$

One can then consider three possible cases: $|Tr(J)| < 2$, $|Tr(J)| > 2$, and $|Tr(J)| = 2$. For $|Tr(J)| < 2$, one obtains $|\lambda_\pm| = 1$ (with $\lambda_\pm \in \mathbb{C}$); one obtains a complex exponential, implying oscillations about zero. Thus, the orbit in question is stable. For $|Tr(J)| > 2$, one obtains real $\lambda_\pm$, with either $|\lambda_+| > 1$ or $|\lambda_-| > 1$. Because $|\lambda_+| > 1$, the deviations grow exponentially and the orbit is unstable. For $|Tr(J)| = 2$, one obtains $\lambda_\pm = 1$ or $\lambda_\pm = -1$, so the orbit is linearly stable [5] (one can also see from the exponential that deviations grow linearly).

For a period k orbit, the Jacobian is

$$J = \prod_{i=1}^{k} F_i C_i, \tag{4}$$

where F_i is the ith free flight matrix (from the travel between collisions) and C_i is the ith collision matrix.

$$F_i = \begin{pmatrix} 1 & L_i \\ 0 & 1 \end{pmatrix} \tag{5}$$

$$C_i = -\begin{pmatrix} 1 & 0 \\ \frac{2}{\rho_i \cos \phi_i} & 1 \end{pmatrix} \tag{6}$$

For billiard systems (for which the confined particles have constant speed 1), L_i is the distance traveled between the $(i-1)$st and the ith collision, ρ_i is the radius of curvature at the ith collision, and ϕ_i is the angle between the outgoing particle and the outward normal at the ith collision.

Poincaré Maps

To examine more complicated orbits, we plot the billiard map (i.e., a Poincaré map) in phase space. The axes are the angle of incidence of collisions and the arc length along the billiard boundary (see Figure 2a).

Each point in phase space corresponds to a collision with the boundary. As mentioned earlier, the points arise from the billiard map. That is, in a phase portrait, one plots the points x_n from iterations of the billiard map. Arc length is measured clockwise from some arbitrarily defined point along the boundary (in this case, the bottom right corner of the cap).

Islands of integrability resemble sets of ellipses around points in phase space that correspond to stable periodic orbits. For example, in Figure 2a, one can see a pink ellipse around $(s, \theta) = (9, 0)$. Figure 2b depicts the configuration space of the same billiard (without trajectories). One can see in Figure 2b that $s \approx 9$ is near the center of the top of the ellipse and that $\theta \approx 0$ is almost perpendicular to the boundary. Thus, the aforementioned pink ellipse in phase space represents a family of trajectories colliding repeatedly against the boundary near the center of the elliptical cap

at nearly perpendicular angles. At the center of this pink ellipse is the point $(s, \theta) = (9, 0)$, which corresponds to the vertical period 2 orbit along the mushroom's axis of symmetry.

One can see another pink circle in phase space centered near $(s, \theta) = (2.5, 0)$. In configuration space, one can see that this corresponds to a family of trajectory bouncing perpendicularly off the center of the bottom of the stem. Together, these two pink ellipses correspond to the same family of trajectories and the centers of these two ellipses together correspond to this period 2 orbit.

Phase portraits are useful for investigating periodic orbits. Certain lower-period orbits obviously exist in some tables (as can be seen using geometric intuition), but most periodic orbits are more difficult to discern. The pink ellipses described previously constitute a pair of "KAM islands" [9], at the centers of which lie a set of points corresponding to periodic orbits. Exploiting such structures allows one to find many complicated periodic orbits from Poincaré maps such as Figure 2a.

While using a previously written graphical user interface (GUI) [1] to generate plots such as Figure 2a, it was sometimes convenient to add functionality so that certain simulations could be done more easily. See Appendix 1 for further details.
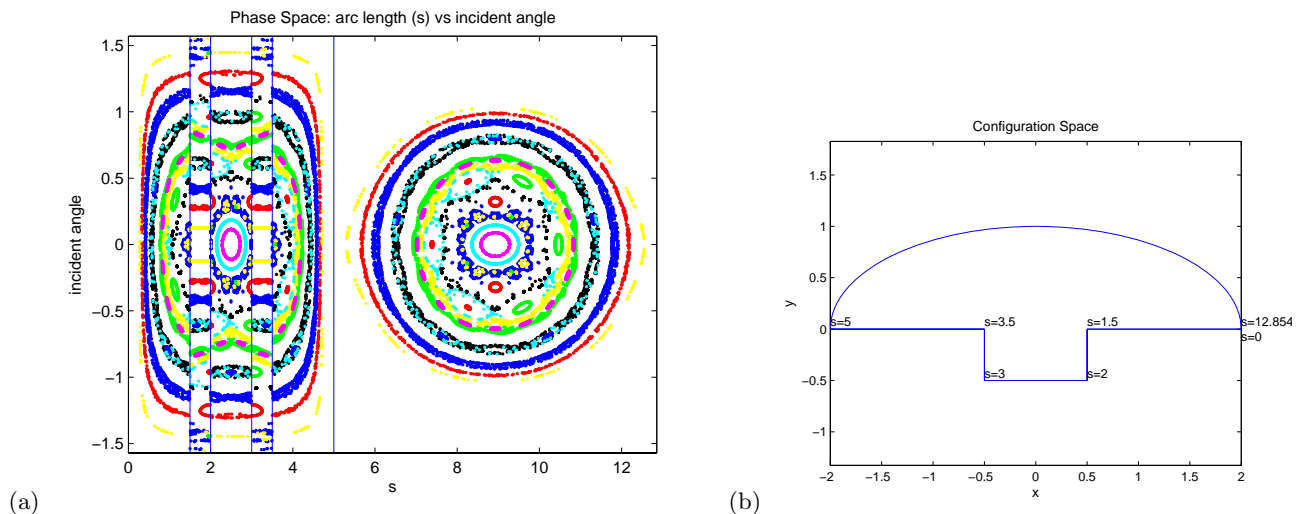

(a)   (b)

FIG. 2: **(a)** Elliptical mushroom billiard phase portrait. The horizontal radius is $r_h = 2$, the vertical radius is $r_v = 1$, the stem width is $w = 1$, the total height is $h = 1.5$, and the quantity s represents the arc length along the boundary. **(b)** Configuration space for the mushroom in (a).

Period 2 Orbits (along the vertical symmetry axis)

Consider again the vertical period 2 orbit in an elliptical mushroom with total height h, stem width w, horizontal cap radius r_h, and vertical cap radius r_v that first hits the center of the cap's top and then the center of its stem . The orbit's period is $k = 2$ because there are two bounces, and the free flight propogation distances are $L_1 = L_2 = h$. The radius of curvature $\rho_1 = \infty$ because the first collision is against a neutral boundary (a straight line), and $\rho_2 = r_h^2 / r_v$ from the definition of curvature and the equation for the ellipse. Additionally, $\phi_1 = \phi_2 = \pi$ because both collisions are perpendicular to the boundary. This yields

$$F_1 = F_2 = \begin{pmatrix} 1 & h \\ 0 & 1 \end{pmatrix}, \tag{7}$$

$$C_1 = -\begin{pmatrix} 1 & 0 \\ 0 & 1 \end{pmatrix},$$

$$C_2 = -\begin{pmatrix} 1 & 0 \\ \frac{-2r_v}{r_h^2} & 1 \end{pmatrix},$$

$$J = F_1 C_1 F_2 C_2 = \begin{pmatrix} 1 - \frac{6hr_v}{r_h^2} + \frac{4h^2 r_v^2}{r_h^4} & 2h(1 - \frac{hr_v}{r_h^2}) \\ \frac{-4r_v(r_h^2 - hr_v)}{r_h^4} & 1 - \frac{2hr_v}{r_h^2} \end{pmatrix},$$

$$Tr(J) = 2 + \frac{4h^2 r_v^2}{r_h^4} - \frac{8hr_v}{r_h^2}.$$

For stability, we need $|Tr(J)| \le 2$. Thus we solve $Tr(J) = 2$:

$$
\begin{align}
2 &= 2 + \frac{4h^2 r_v^2}{r_h^4} - \frac{8hr_v}{r_h^2}, \tag{8} \\
0 &= \frac{4h^2 r_v^2}{r_h^4} - \frac{8hr_v}{r_h^2}, \\
0 &= \frac{h^2 r_v^2}{r_h^4} - \frac{2hr_v}{r_h^2}, \\
0 &= \frac{hr_v}{r_h^2}(\frac{hr_v}{r_h^2} - 2), \\
\frac{hr_v}{r_h^2} &= 2, \\
h &= \frac{2r_h^2}{r_v}.
\end{align}
$$

We also solve $Tr(J) = -2$:

$$
\begin{align}
-2 &= 2 + \frac{4h^2 r_v^2}{r_h^4} - \frac{8hr_v}{r_h^2}, \tag{9} \\
-4 &= \frac{4h^2 r_v^2}{r_h^4} - \frac{8hr_v}{r_h^2}, \\
-1 &= \frac{h^2 r_v^2}{r_h^4} - \frac{2hr_v}{r_h^2}, \\
0 &= (\frac{hr_v}{r_h^2} - 1)^2, \\
\frac{hr_v}{r_h^2} &= 1, \\
h &= \frac{r_h^2}{r_v}.
\end{align}
$$

The equation $Tr(J) = 2$ yields $h = 2r_h^2/r_v$ and $Tr(J) = -2$ yields $h = r_h^2/r_v$. Testing these conditions numerically, we see that the orbit is stable for $h < r_h^2/r_v$. Similar calculations for the double mushroom (the main difference in the calculations is that $\rho_1 = \rho_2 = r_h^2/r_v$) yield a similar condition for stability: $h < 2r_h^2/r_v$.

We confirm these results using the parameter values $r_h = 2$, $r_v = 1$, and $w = 1$ in the single elliptical mushroom with numerical computations of the eigenvalues (see Figure 3a). See Appendix 2 for more details on eigenvalue plotting. For $h < 4$, the magnitudes of the eigenvalues are 1, so the orbit is stable. This plot confirms our result, as the orbit is stable for $h < r_h^2/r_v = 4$.
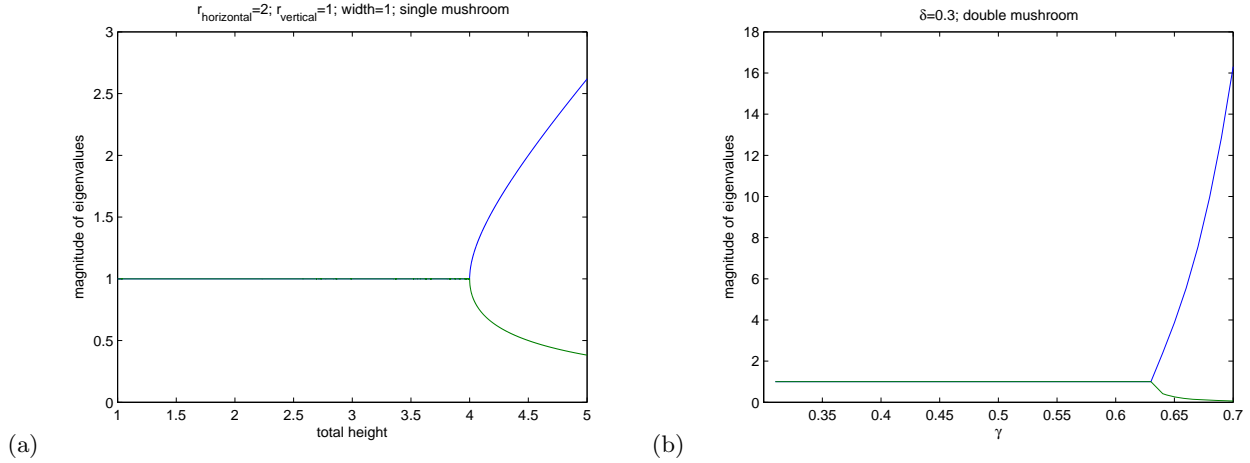
FIG. 3: **(a)** Elliptical mushroom billiard eigenvalue plot for period-2 orbit. The orbit becomes unstable at $h = 4$. The quantity $r_{horizontal}$ is the horizontal radius of the semi-elliptical cap, $r_{vertical}$ is the vertical radius of the semi-elliptical cap, and "width" and "height" refer to the stem size. **(b)** Elliptical stadium billiard eigenvalue plot for period-4 bowtie orbit with $\delta = .3$. The orbit becomes unstable $\gamma \approx .63$. the quantity 2δ is the stem height, γ is the stem width and the horizontal radius, and $1 - \delta$ is the vertical radius.

Diamond Orbits

Our motivation for investigating diamond orbits was a study on similar orbits in stadium billiards with elliptical caps [2].

Period 4

In an elliptical mushroom with total height h, stem width w, horizontal cap radius r_h, and vertical cap radius r_v, consider the period 4 diamond orbit that hits the cap, as seen in Figure 1b. Without loss of generality, we will do our calculations for the case in which it is traveling clockwise. Hence, $k = 4$ because there are 4 bounces, and $L_1 = L_2 = L_3 = L_4 = \frac{1}{4}\sqrt{h^2 + w^2}$. Moreover $\rho_1 = r_h^2/r_v$ and $\rho_2 = \rho_3 = \rho_4 = \infty$, as the collisions are against neutral boundaries. Additionally, $\phi_1 = \phi_3 = \pi/2 + \arctan(h/w)$ and $\phi_2 = \phi_4 = \pi/2 + \arctan(w/h)$. This yields

$$F_1 = F_2 = F_3 = F_4 = \begin{pmatrix} 1 & h \\ 0 & 1 \end{pmatrix}, \tag{10}$$

$$C_1 = -\begin{pmatrix} \frac{1}{\frac{2}{(r_h^2/r_v)\cos(\pi/2+\arctan(h/w))}} & 0 \\ & 1 \end{pmatrix} = -\begin{pmatrix} 1 & 0 \\ \frac{2r_v\sqrt{w^2+h^2}}{hr_h^2} & 1 \end{pmatrix},$$

$$C_2 = C_3 = C_4 = -\begin{pmatrix} 1 & 0 \\ 0 & 1 \end{pmatrix},$$

$$J = \frac{1}{hr_h^2}\begin{pmatrix} hr_h^2 - 6r_v(h^2 + w^2) & -2\sqrt{h^2 + w^2}(-2hr_h^2 + 3h^2 r_v + 3r_v w^2) \\ -2r_v\sqrt{h^2 + w^2} & hr_h^2 - 2r_v(h^2 + w^2) \end{pmatrix},$$

$$Tr(J) = 2 - \frac{8r_v(h^2 + w^2)}{hr_h^2}.$$

Solving $|Tr(J)| = 2$, we find that the orbit is stable when $r_v < (hr_h^2)/(h^2 + w^2)$. Similar calculations (the main difference is that $\rho_1 = \rho_3 = r_h^2/r_v$) yield the stability condition for the double mushroom: $r_v < (2hr_h^2)/(h^2 + w^2)$. We confirmed this result with a numerical check in the billiard simulator GUI.

Period 2n

Generalizing from period 4 to period $2n$ entails incorporating extra bounces along the side of the stem. The calculations are similar, yielding the stability condition $r_v < (hr_h^2)/(h^2 + (n-1)^2 w^2)$ for the single mushroom and $r_v < (2hr_h^2)/(h^2 + (n-1)^2 w^2)$ for the double mushroom.

Bowtie Orbits

As with diamond orbits, our work on bowtie orbits is motivated by the study of similar orbits in elliptical stadia [2]. We show an example of a period 4 bowtie orbit in Figure 1b. A related orbit exists in the single mushroom, due to the reflection symmetry about the horizontal axis through the stem of the double mushroom. This related orbit hits the cap twice and the center of the stem once.

Because the analytical computations for these orbits are extremely tedious, we restrict our attention to numerical calculations by examining the eigenvalues of the Jacobian matrix for different values of the table parameters. In studying the bowtie orbit, we sometimes work with the elliptical stadium for two reasons. First, one obtains the same orbit because the trajectory does not include collisions with the side of the stem. Second, the stadium is simpler to use because it can be characterized by fewer parameters. In working with the stadium, we adopt the parameter conventions in [2]. That is, the total height is $h = 2$ (which is fixed without loss of generality), the horizontal cap radius is $r_h = \gamma$, and the vertical cap radius is $r_v = 1 - \delta$ (this notation is used in place of r_h, r_v, and h). Figure 3b shows a plot of the eigenvalues for $\delta = .3$, for which the orbit becomes unstable when $\gamma \approx .63$.

Diamond Sizes

With many periodic orbits, diamonds form where the orbits cross themselves. In a period-4 diamond orbit (see Figure 1b), there is one diamond. For higher-period diamond orbits, there are many diamonds (of the same size) instead of one. More complicated orbits can, however, have diamonds of many different sizes (see Figure 4a). We consider the sizes of these diamonds (particularly those in and near the stem) as the period increases.

We initially thought that there would be some sort of general relation for diamond sizes of periodic orbits and hypothesized that the size and period were inversely proportional. While this is true for diamond orbits (such as the type in Figure 1b), it does not hold in general. One unanticipated issue is that an orbit can bounce many more times in the cap than in the stem and that the number of bounces in the cap can be largely unrelated to the characteristic diamond size (see Figure 4).

We plotted diamond size versus period for a particular class of periodic orbits whose trajectories are perpendicular to the semi-ellipse in the cap at some point (see Figure 5a). We sweep an interval of initial x-coordinates where the trajectory is perpendicular to the cap and then check whether the trajectory is a periodic orbit. If so, we calculate the diamond size and period (see Figure 5b).

One known issue with this is that the code expects the orbit to alternate between hitting the semi-elliptical part of the cap and the neutral part of the cap before entering the stem; considering a trajectory which hits the semi-ellipse two or more times in a row can lead to spurious data.

We also examined rounded mushrooms, which have quarter circles in place of corners where the stem meets the cap. However, the code had problems handling trajectories that hit the quarter circles or came near them. We fixed some related bugs, but there remain unresolved issues concerning false data in such plots.

CONCLUSION

We obtained analytical and numerical results for the stability of various orbits in elliptical mushroom billiards – including the period 2 orbit through the vertical axis of symmetry, period 4 diamond orbits, and period $2n$ diamond orbits. We also obtained numerical stability results for bowtie orbits and studied the size of the "diamonds" in
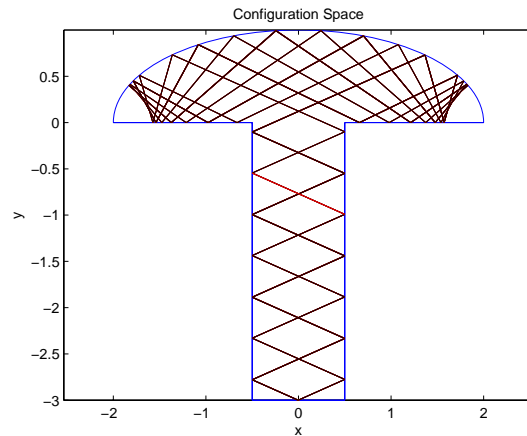
FIG. 4: A period 88 orbit with almost all of the collisions in the cap of an elliptical mushroom with $h = 4$, $r_h = 2$, $r_v = 1$, $w = 1$.

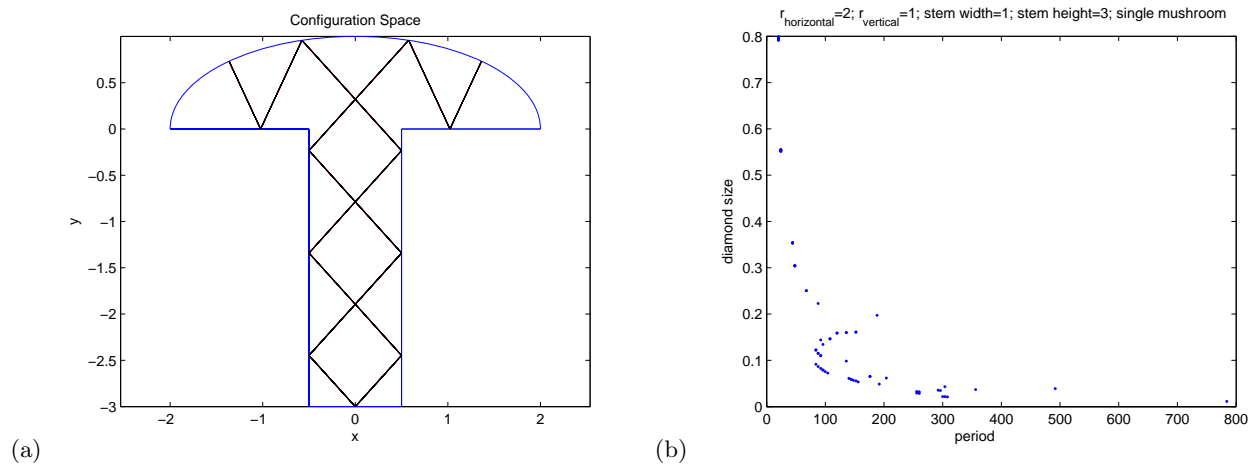(a)   (b)

FIG. 5: **(a)** Period 24 orbit with a trajectory that is perpendicular to the cap in the same billiard as figure 4. We studied the diamond sizes of this orbit and other orbits with such perpendicular collisions. **(b)** Diamond sizes for the billiard and class of orbits shown in (a). Each point on the graph represents a periodic orbit plotted by its period and diamond size.

configuration space that one sees with periodic orbits.

The study of simple mixed systems such as mushroom billiards can lead to a better understanding of mixed systems, which in general are very difficult to analyze thoroughly. We studied the particular case of single and double elliptical mushrooms. Our further investigation of these such systems will include studies of the relation between diamond size and period, the stability of higher-period orbits of various classes, and symbolic dynamics.

My studies were partly focused on generalizing the results of [2] to mushrooms and double mushroom billiards. As

such, I would like to thank the authors of that paper. Additionally, private correspondance with V. Lopać (one of the authors of [2]) was useful.

APPENDIX 1 - WORK DONE ON THE GUI

We conducted some numerical studies in a Matlab graphical user interface (GUI) for billiard simulation [1]. We added functionality to the GUI in a few different ways. We added 5 new tables (double mushroom, non-concentric circles, rounded mushroom, Kaplan Billiard [14], and lemon billiard [13]), which are customizable and available for use in simulations. Additionally, we expanded the stadium billiard option, which can now be used for either circular or elliptical stadia rather than only circular ones.

We added an extra mode for plotting phase portraits: s vs $|\theta|$, where s is the arc length and θ is the incident angle. Typically, KAM islands can be difficult to find using the GUI's phase portraits (of s vs θ) unless one simulates trajectories for many collisions. One reason is that a trajectory colliding with the boundary at (s, θ) is treated differently from a collision with the boundary at $(s, -\theta)$, despite the fact that these two trajectories are simply time-reversed. Thus, by instead plotting s vs $|\theta|$, the data appears denser and KAM islands become easier to observe.

APPENDIX 2 - EIGENVALUE PLOTTING CODE

The primary purpose of this code is to plot the eigenvalues of the Jacobian matrix for some periodic orbit as one parameter describing the table is varied. As discussed in the main text, the magnitudes of eigenvalues are used to determine stability, so these plots are very useful for supplementing analytical calculations of stability.

We wrote this code so that we can easily fix parameters of my choice while varying another, which is ideal for obtaining these plots under many different conditions. This code relies on two parts. The first is a file that calculates the Jacobian for an orbit given a specific table. This calculation of the Jacobian must be coded by the user for each periodic orbit. The second part, which works with minimal modifications for any table and orbit, collects data from the first part and plots it.

[1] Steven Lansel and Mason A. Porter. A Graphical User Interface to Simulate Classical Billiard Systems. nlin.CD/0405033 (2004).

[2] V. Lopać, N. Pavin Mrkonijic, N. Pavin, and D. Radić. Chaotic Dynamics of the Elliptical Stadium Billiard in the Full Parameter Space, *Physica D*. Vol. 217, No. 1 (2006), 88 − 101.

[3] Steven H. Strogatz. *Nonlinear Dynamics and Chaos*. Addison-Wesley: Reading, 1994.

[4] P. Cvitanović, R. Artuso, R. Mainieri, G. Tanner and G. Vattay. *Chaos: Classical and Quantum*, ChaosBook.org. Niels Bohr Institute: Copenhagen, 2005.

[5] M. V. Berry. Regularity and Chaos in Classical Mechanics, Illustrated by Three Deformations of a Circular Billiard, *European Journal of Physics*. Vol. 2, No. 2 (1981), 91 − 102.

[6] Leonid A. Bunimovich. Mushrooms and Other Billiards with Divided Phase Space, *Chaos*. Vol. 11, No. 1 (2001), 802 − 808.

[7] Steven Lansel, Mason A. Porter, and Leonid A. Bunimovich. One-Particle and Few-Particle Billiards, *Chaos*. Vol. 16, No. 1, Article 013129 (2006).

[8] Ya. G. Sinai. WHAT IS...a billiard, *Notices of the American Mathematical Society*. Vol. 51, No. 4 (2004), 412 − 413.

[9] Mason A. Porter and Steven Lansel. Mushroom Billiards, *Notices of the American Mathematical Society*. Vol. 53, No. 3 (2006), 334 − 337.

[10] Y. Okada, A. Shudo, S. Tasaki and T. Harayama. 'Can One Hear The Shape of a Drum?': Revisited, *Journal of Physics A: Mathematical and General*. Vol. 38, No. 9 (2005), 163 − 170.

[11] N. Friedman, A. Kaplan, D. Carasso, and N. Davidson. Observation of chaotic and regular dynamics in atom-optics billiards, *Physical Review Letters*. Vol. 86, No. 8 (2001), 1518 − 1521.

[12] A. Kudrolli, V. Kidambi, and S. Sridhar. Experimental Studies of Chaos and Localization in Quantum Wave Functions, *Physical Review Letters*. Vol. 75, No. 5 (1995), 822 − 825.

[13] V. Lopać, I. Mrkonjić, and D. Radić. Chaotic Behavior in Lemon-shaped Billiard with Elliptical and Hyperbolic Boundary Arcs, *Physical Review E*. Vol. 64, No. 1, Article 016214 (2001).

[14] L. Kaplan and and E. J. Heller. Short-time effects on eigenstate structure in Sinai billiards and related systems, *Physical Review E*. Vol. 62, No. 1 (2000), 409 – 426.